Crystal growth kinetics of Sb$_2$S$_3$ in Ge–Sb–S amorphous thin films

Jaroslav Barták · Jiří Málek

Abstract Sb$_2$S$_3$ crystal growth kinetics in $(GeS_2)_x$ $(Sb_2S_3)_{1-x}$ thin films ($x = 0.4$ and 0.5) have been investigated through this study by optical microscopy in the temperature range of 575–623 K. Relative complex crystalline structures composed of submicrometer-thin Sb$_2$S$_3$ crystal fibers develop linearly with time. The data on temperature dependence of crystal growth rate exhibit an exponential behavior. Corresponding activation energies were found to be $E_G = 279 \pm 7$ kJ mol^{-1} for $x = 0.4$ and $E_G = 255 \pm 5$ kJ mol^{-1} for $x = 0.5$. These values are similar to activation energies of crystal growth in bulk glasses of the same compositions. The crystal growth is controlled by liquid–crystal interface kinetics. It seems that the 2D surface-nucleated growth is operative in this particular case. The calculated crystal growth rate for this model is in good agreement with experimental data. The crystal growth kinetic characteristic is similar for both the bulk glass and thin film for $x = 0.4$ composition. However, it differs considerably for $x = 0.5$ composition. Thermodynamic and kinetic aspects of crystal growth are discussed in terms of Jackson's theory of liquid–crystal interface.

Keywords Crystal growth · Thin films · Ge–Sb–S · Optical microscopy

Introduction

Antimony trisulfide (Sb$_2$S$_3$) with an orthorhombic crystalline structure is an important semiconductor that has many potential applications, such as solar energy conversion, thermoelectric cooling technologies, optoelectronics in the IR region, and photocatalysis. A considerable effort has been devoted to crystal growth control of hierarchical spheroidal crystalline structures of Sb$_2$S$_3$ in solution [1]. Simple 1D crystalline nanostructures, such as nanorods, nanowires, nanotubes, and nanoribbons, as well as some more complex assemblies as 2D nanorod bundles and 3D sheaf-like crystals, were also prepared under controlled growth using hydrothermal route [2].

Another interesting way by which kinetics of crystal growth is controlled involves glassy media or highly supercooled glass-forming liquid. Crystallization kinetics in some compositions of Ge–Sb–S bulk and ground glasses, particularly along the pseudobinary composition line of $(GeS_2)_x(Sb_2S_3)_{1-x}$, has been studied quite intensively by means of DTA [3–6], DSC [7–9], and thermomechanical analysis [10–12]. The influence of particle size distribution of ground glassy samples on the crystallization kinetics has been studied in $(GeS_2)_{0.1}(Sb_2S_3)_{0.9}$ composition [13]. The combined method of kinetic analysis and the invariant kinetic method of analysis of crystallization data have been applied for $(GeS_2)_{0.3}(Sb_2S_3)_{0.7}$ glass [14, 15]. Recently, some studies reporting results of direct measurement of Sb$_2$S$_3$ crystal growth kinetics by means of optical microscopy in bulk glasses of $(GeS_2)_x(Sb_2S_3)_{1-x}$ system have been published [11, 12, 16–19].

From these previous studies, it seems evident that the crystallization process starts predominantly within the bulk of annealed glass, and the crystals grow from randomly distributed nuclei. The morphology of growing crystals is dependent on composition of bulk glass and, in some cases; it also depends on the temperature [16–19]. The length of Sb$_2$S$_3$ single crystal or the diameter of crystalline aggregate increases linearly with time at any selected temperature

J. Barták (✉) · J. Málek
Department of Physical Chemistry, Faculty of Chemical Technology, University of Pardubice, Studentská 95, Pardubice 532 10, Czech Republic
e-mail: j-bartak@seznam.cz

within the range observable by optical microscopy. This type of behavior is typical for crystal growth controlled by crystal–liquid interface kinetics.

The aim of this article is to study crystal growth kinetics of Sb_2S_3 for selected compositions of thin films in $(GeS_2)_x(Sb_2S_3)_{1-x}$ system. The experimental kinetic data obtained by optical microscopy will be compared with the previously published results for the bulk glasses and discussed in terms of standard theory of crystal growth.

Experimental

The $(GeS_2)_x(Sb_2S_3)_{1-x}$ glasses were prepared by synthesis from pure elements (5 N purity). A mixture of these elements (7 g total weight) was placed in silica ampoule (inner diameter, 13 mm; and length, 80 mm). The ampoule was then evacuated to a pressure of 10^{-4} Pa, sealed, and placed in a rotary furnace. After heat treatment and homogenization at 1,223 K for 20 h, the ampoule was rapidly cooled in ice water. The amorphous nature of quenched bulk glass was examined by X-ray diffraction analysis (XRD). These bulk samples were used as starting materials for thin film's preparation. Thin films of $x = 0.4$ and $x = 0.5$ compositions were prepared by thermal evaporation of bulk material of the same composition in high vacuum (2.10^{-4} Pa) on the microscopy glass substrate. During the deposition process, the substrates were conveniently rotated by means of planetary rotation system to ensure high homogeneity of the film thickness. The deposition rate was 1–2 nm/s, measured continuously using the quartz microbalance technique. The final thickness of the prepared films was 1 μm. The composition of prepared films was determined by energy dispersive X–ray (EDX) microanalyser and correlated well with bulk composition.

Optical measurement of crystal growth was performed by using Olympus BX51 microscope on thin films of $(GeS_2)_x(Sb_2S_3)_{1-x}$ composition. These samples were previously heat-treated in a computer-controlled furnace at selected temperatures for various times (central hot zone constant to within ± 0.5 °C) at temperatures where the optimum crystal growth rates are observed. All samples of

thin films were optically transparent and, therefore, the crystal growth rate measurements could be measured in transmission mode. This is a big advantage in comparison with bulk samples of the same composition where in some case the reflectivity measurement should be used instead [10, 14, 17]. All heat-treated samples were extensively examined, and the sizes of the well-developed crystals grown in thin films were measured and recorded.

XRD analysis of amorphous and crystallized sample was performed using a Bruker AXS X-ray diffractometer equipped with horizontal goniometer and scintillation counter, utilizing Ni-Filtered CuK_α radiation (40 kV, 30 mA). The scans were taken over scattering angles, 2θ from 5° to 100° at the low scanning speed of 0.6°/min. The composition of partially crystallized samples was analyzed using energy dispersive electron microanalyser KEVEX coupled with the scanning electron microscope (SEM).

Results

It has been found that the crystallization of Sb_2S_3 in $(GeS_2)_x(Sb_2S_3)_{1-x}$ thin films start within the volume of thin film and is not initiated at the surface. It seems that the crystals start to grow from randomly distributed nuclei. The morphology of growing crystals depends on the thin film composition as shown in Fig. 1. For both the compositions examined (i.e., $x = 0.4$ and $x = 0.5$) crystalline structures exhibit more complex forms that are composed of bundles of submicrometer thin Sb_2S_3 crystals. These crystalline aggregates form relatively compact assemblies for $x = 0.4$ composition, while a more opened structures are found for $x = 0.5$ composition. All these crystalline aggregates grow linearly with time as shown in Fig. 2. This type of behavior is typical for crystal growth controlled by interface kinetics.

It should be pointed out that there are some experimental constraints for crystal size measurement. Although it is principally possible to observe micrometer-sized crystals in amorphous thin films by optical microscopy for a reliable measurement, we need to measure multiple crystalline objects and then calculate average crystal sizes. From this point of view, the minimum measurable size by

Fig. 1 Photographs of partially crystallized samples of thin films of $(GeS_2)_x(Sb_2S_3)_{1-x}$ composition: **a** $x = 0.4$, $T = 599.6$ K, $t = 90$ min, polarized light; **b** $x = 0.5$, $T = 612.5$ K, $t = 210$ min, transmitted light
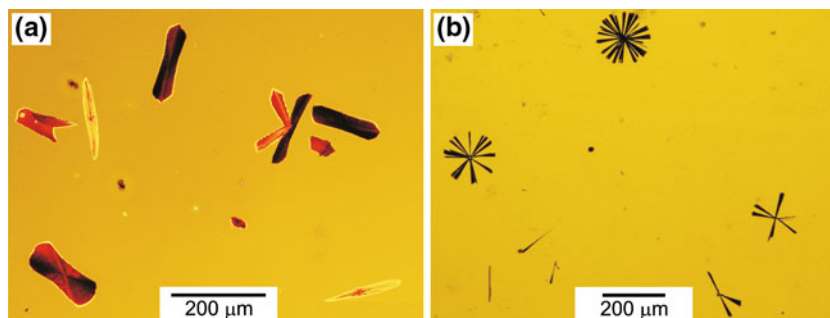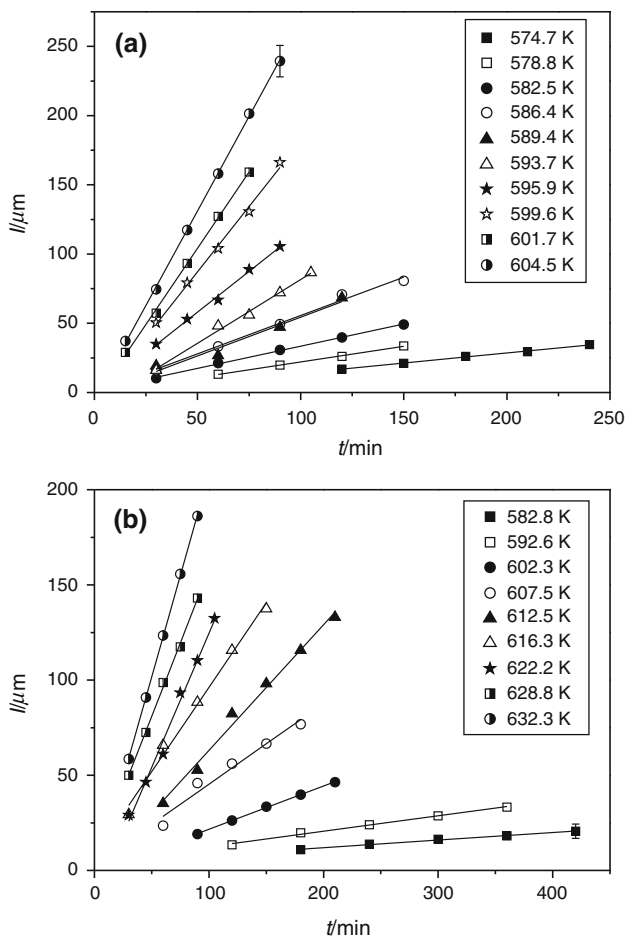
Fig. 2 Time dependence of the length of Sb$_2$S$_3$ crystalline aggregates grown in thin films of $(GeS_2)_x(Sb_2S_3)_{1-x}$ composition: **a** $x = 0.4$; **b** $x = 0.5$. Experimental errors of crystal lengths are indicated by *error bars* for the lowest and the highest crystal growth rate

Table 1 Crystal growth rates in $(GeS_2)_x(Sb_2S_3)_{1-x}$ thin films

$x = 0.4$		$x = 0.5$	
T/K	$u/\mu m\ min^{-1}$	T/K	$u/\mu m\ min^{-1}$
574.7	0.16 ± 0.02	582.7	0.042 ± 0.005
578.8	0.24 ± 0.02	592.6	0.10 ± 0.01
582.5	0.33 ± 0.02	602.3	0.26 ± 0.04
586.4	0.55 ± 0.03	607.5	0.36 ± 0.04
589.4	0.74 ± 0.06	612.5	0.60 ± 0.04
593.7	0.93 ± 0.08	616.3	0.88 ± 0.08
595.9	1.18 ± 0.07	622.2	1.3 ± 0.1
599.6	1.9 ± 0.1	623.4	1.3 ± 0.1
601.7	2.2 ± 0.2	628.4	1.82 ± 0.07
604.5	2.8 ± 0.2	632.3	2.5 ± 0.2

thin films of $x = 0.4$ and $x = 0.5$ compositions. Straight line dependence is indicative of simple exponential growth rate behavior in this limited temperature range. Activation energies of crystal growth for both compositions were calculated from the slopes of these linear dependences as follows: $E_G = 279 \pm 7$ kJ mol^{-1} for $x = 0.4$, and $E_G = 255 \pm 5$ kJ mol^{-1} for $x = 0.5$. These values are close to activation energies of crystal growth of Sb$_2$S$_3$ in bulk glasses of the same compositions reported previously: Zmrhalová et al. [12] found $E_G = 274 \pm 7$ kJ mol^{-1} for bulk sample of $x = 0.4$ composition, and Švadlák [19] found $E_G = 293 \pm 3$ kJ mol^{-1} for bulk sample of $x = 0.5$ compositions. Owing to relatively slow nucleation-growth process, it is difficult to experimentally observe a reproducible crystallization peak by conventional thermal analysis methods. It is probable that the heat flow associated with crystallization is below the signal-to-noise ratio typical for these methods. Therefore, the activation energies for crystal growth
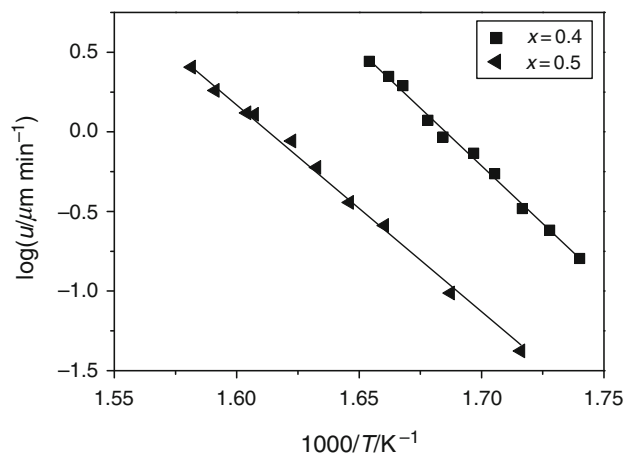
optical microscopy is around 6 μm. Similarly, there is a maximum limit of crystal size because of some spatial constraints and crystal impingements influencing later growth stages. The maximum measurable size of crystalline structures in thin films of $x = 0.4$ and 0.5 compositions is around 240 μm. Data shown in Fig. 2 correspond to these experimental limits. Any data point is calculated as an average of 50–60 measurements of different crystalline objects found in the thin film annealed at a selected temperature. Solid lines correspond to a least-squares fit to these data. The slope of linear time dependence of crystal size at any temperature corresponds to crystal growth rate. These results are summarized in Table 1.

Discussion

Figure 3 shows the crystal growth rate data given in Table 1 as a function of reciprocal temperature for $(GeS_2)_x(Sb_2S_3)_{1-x}$

Fig. 3 Temperature dependence of crystal growth rate in amorphous films of $(GeS_2)_x(Sb_2S_3)_{1-x}$ composition. *Points* correspond to experimental data. *Solid line* was calculated by linear regression

obtained by microscopic measurement cannot be compared with activation energies of nucleation-growth process obtained by DSC experiments as was done previously for $x \leq 0.3$ compositions [16–18].

As has been anticipated above, it seems that the crystal growth is controlled by liquid–crystal interface kinetics. The crystalline aggregates composed of bundles of sub-micrometer thin Sb_2S_3 crystals grow linearly with time. Sb_2S_3 has relatively high entropy of fusion (5.94 R), which according to Jackson's theory [21], corresponds to faceted crystal–liquid interface. A complex structure of crystalline aggregates of Sb_2S_3, somewhat resembling sections of spherulites composed of thin crystal fibers, can be explained in this way.

There are three basic phenomenological models suitable for description of crystal growth controlled by interface kinetics: normal growth, screw dislocation growth, and 2D surface-nucleated growth [20]. The operative growth mechanism can be assessed from the reduced growth rate U_R [21]:

$$U_R = \frac{u\,\eta}{1 - \exp\left(-\frac{\Delta S_f \Delta T}{R\,T}\right)} \tag{1}$$

where T is the temperature at which the crystal growth rate u and the viscosity η are measured; ΔT is the undercooling with respect to the melting point ($\Delta T = T_m - T$); and ΔS_f is entropy of fusion of the crystalline phase. Therefore, for normal growth, the U_R versus ΔT should be a horizontal line, and for screw dislocation growth, where the interface site factor is linearly temperature dependent, this plot is expected to be a straight line of positive slope passing through the origin. In contrast, for 2D surface-nucleated growth, U_R versus ΔT plot should be in form of a curve of increasing positive slope passing through the origin.

To calculate the $U_R(\Delta T)$ dependence from our experimental data, the values of ΔS_f and T_m for Sb_2S_3 crystals and viscosity of undercooled melt of our samples are needed. Johnson et al. [22] reported these values to be $\Delta S_f/R = 5.94 \pm 0.03$ and $T_m = 823$ K. Shánělová et al. [23] measured viscosity of $(GeS_2)_x(Sb_2S_3)_{1-x}$ supercooled bulk melts in temperature range that is close to our crystal growth experiments. These data were used in calculations that are to follow. Therefore, it is assumed that viscosity of supercooled liquid corresponding to a thin film is essentially the same as for bulk glasses. Figure 4 shows the reduced crystal growth rate for both compositions of $(GeS_2)_x(Sb_2S_3)_{1-x}$ thin films. The positive curvature of this plot suggests the 2D surface-nucleated growth. According to Uhlmann et al. [20], the crystal growth rate can be expressed as

$$u = \frac{C}{\eta}\exp\left(-\frac{B}{T\,\Delta T}\right) \tag{2}$$

where B and C are parameters of the model. The constants B and C were obtained from the linear dependence of

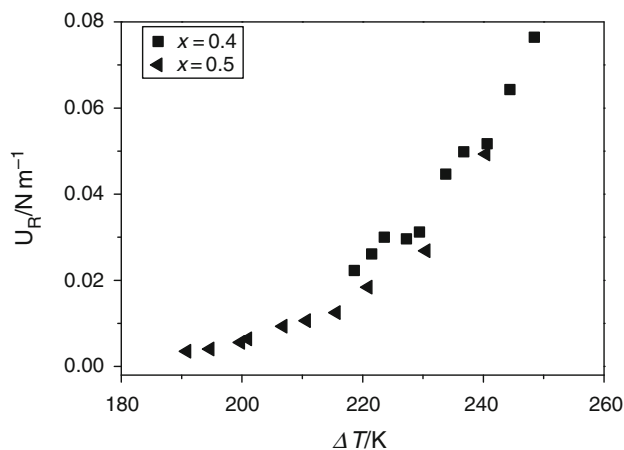**Fig. 4** Reduced growth rate versus supercooling for crystallization of Sb_2S_3 in thin films of $(GeS_2)_x(Sb_2S_3)_{1-x}$ composition

$\ln(u\eta)$ versus $1/(T\Delta T)$ shown in Fig. 5. It is seen that the dependence for the crystal growth of Sb_2S_3 predicted by Eq. 2 is confirmed in the whole temperature range. The parameters of the 2D surface-nucleated models were obtained from the linear fit and are listed in Table 2.

Figure 6 shows temperature dependences of crystal growth rate of Sb_2S_3 in $(GeS_2)_x(Sb_2S_3)_{1-x}$ for thin films and bulk samples [12, 19]. The points correspond to experimental data (Table 1), and the lines (solid and broken) were calculated by Eq. 2 for parameters given in Table 2 and reported viscosity data [23]. It is seen the calculated crystal growth rates are in good agreement with experimental data. However, the crystal growth rates of bulk glass and thin film are similar for $x = 0.4$ composition. In contrast, the crystal growth rate is considerably higher in thin film than in bulk glass for $x = 0.5$ composition. These changes are reflected in the value of kinetic parameter C
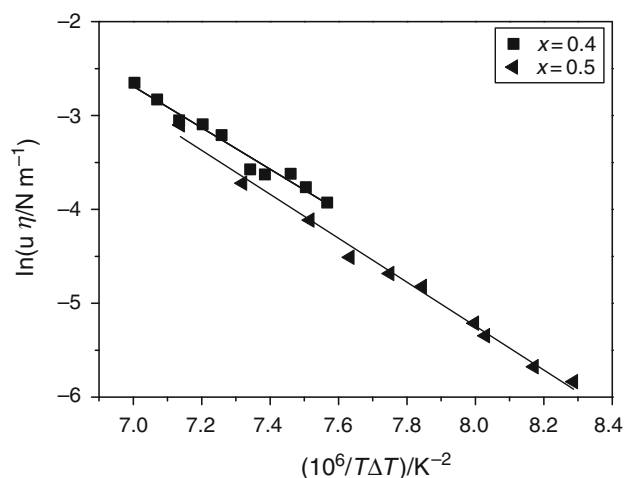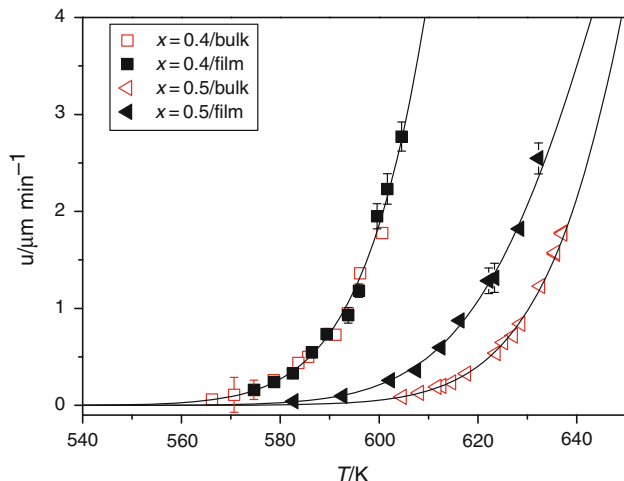

Fig. 5 Plot of logarithm (growth rate × viscosity) versus $1/(T\Delta T)$ for crystallization of Sb_2S_3 in $(GeS_2)_x(Sb_2S_3)_{1-x}$ thin films. The *solid lines* correspond to the linear regression

Table 2 Values of parameters of 2D surface-nucleated crystal growth model in $(GeS_2)_x(Sb_2S_3)_{1-x}$ thin films

	$x = 0.4$	$x = 0.5$
$B/10^6$ K^{-2}	2.2 ± 0.1	2.3 ± 0.1
$\ln (C/\text{N m}^{-1})$	12.8 ± 1.0	13.5 ± 0.6

Fig. 6 Temperature dependence of crystal growth rate of Sb$_2$S$_3$ in $(GeS_2)_x(Sb_2S_3)_{1-x}$ thin films and bulk glasses [12, 19]. *Solid lines* correspond to 2D surface-nucleated growth model calculated by Eq. 2

that changes considerably with composition as well as for bulk and thin film. In contrast, the value of parameter B seems to be practically constant (at least within the limits of combined experimental errors) for thin films (see Table 2). This parameter can be expressed as [20]

$$B = \frac{\pi \lambda V_m \sigma_E^2}{3 k \Delta S_f} \tag{3}$$

where k is the Boltzmann constant. The entropy of fusion, ΔS_f, the diameter of Sb$_2$S$_3$ molecule, λ, and the molar volume of crystallized substance, V_m are identical for both the compositions of thin film. Therefore, the parameter B is proportional to σ_E^2, that is, the edge surface free energy of nucleus should be equivalent to the liquid–crystal surface tension, provided there is no marked change in surface structure associated with deformation [24]. It seems that this thermodynamic parameter characterizing liquid–crystal interface in $(GeS_2)_x(Sb_2S_3)_{1-x}$ system is practically constant for the thin films of compositions $0.4 \leq x \leq 0.5$ (see Table 2). The value of parameter B for the bulk samples was found to be 2.5×10^6 K^{-2} for $x = 0.4$ composition [12] and 1.5×10^6 K^{-2} for $x = 0.5$ composition [19].

Conclusions

It has been found that $(GeS_2)_x(Sb_2S_3)_{1-x}$ thin films ($x = 0.4$ and $x = 0.5$ compositions) crystallize in temperature range

575–623 K as a more complex crystalline structures that are composed of bundles of submicrometer thin Sb$_2$S$_3$ crystals. Within this temperature range, the crystal growth rate data can be described by an exponential behavior. Corresponding activation energies were found to be $E_G = 279 \pm 7$ kJ mol^{-1} ($x = 0.4$) and $E_G = 255 \pm 5$ kJ mol^{-1} ($x = 0.5$). These values are similar to activation energies of crystal growth in bulk glasses of the same compositions.

The crystal growth is controlled by liquid–crystal interface kinetics. It seems that the 2D surface-nucleated growth is operative in this particular case. The calculated crystal growth rate for this model is in good agreement with experimental data. The crystal growth kinetics is similar for the bulk glass and thin film for $x = 0.4$ composition. However, it differs considerably for $x = 0.5$ composition.

References

1. Pan J, Xiong S, Xi B, Li J, Li J, Zhou H, Qian Y. Tartaric Acid and L–cysteine synergistic–assisted synthesis of antimony trisulfide hierarchical structures in aqueous solution. Eur J Inorg Chem. 2009:5302.
2. Ma J, Duan X, Lian J, Kim T, Peng P, Liu X, Liu Z, Li H, Zheng W. Sb$_2$S$_3$ with various nanostructures: controllable synthesis, formation mechanism, and electrochemical performance toward lithium storage. Chem Eur J. 1010;16:13210.
3. Ryšavá N, Tichý L, Barta Č, Tříska A, Tichá H. Kinetics recrystallization of Sb$_2$S$_3$ in glassy $(GeS_2)_{0.3}(Sb_2S_3)_{0.7}$. Phys Status Solidi A. 1985;87:K13.
4. Ryšavá N, Spasov T, Tichý L (1987) Isothermal DSC method for evaluation of the kinetics of crystallization in the Ge–Sb–S glassy system. J Therm Anal. 32: 1015.
5. Ryšavá N, Barta Č, Tichý L. On the crystallization of Sb$_2$S$_3$ in glassy $(GeS_2)_{0.3}(Sb_2S_3)_{0.7}$. J Mat Sci Lett. 1989;8:91.
6. Málek J, Smrčka V. The kinetic analysis of the crystallization processes in glasses. Thermochim Acta. 1991;186:153.
7. Málek J, Černošková E, Švejka R, Šesták J, Van der Plaats G. Crystallization kinetics of Ge$_{0.3}$Sb$_{1.4}$S$_{2.7}$ glass. Thermochim Acta. 1996;280–281:353.
8. Málek J. Crystallization kinetics by thermal analysis. J Therm Anal Calorim. 1999;56:763.
9. Málek J. Kinetic analysis of crystallization processes in amorphous materials. Thermochim Acta. 2000;355:239.
10. Málek J, Zmrhalová Z, Barták J, Honcová P. A novel method to study crystallization of glasses. Thermochim Acta. 2010;511:67–73.
11. Málek J, Zmrhalová Z, Honcová P. Crystallization in glasses monitored by thermomechanical analysis. J Therm Anal Calorim. 2011;105:565.
12. Zmrhalová Z, Málek J, Švadlák D, Barták J. The crystallization kinetics of Sb$_2$S$_3$ in $(GeS_2)_{0.4}(Sb_2S_3)_{0.6}$ glass. Phys Status Solidi C. 2011;8:3127.
13. Pustková P, Zmrhalová Z, Málek J. The particle size influence on crystallization kinetics of $(GeS_2)_{0.1}(Sb_2S_3)_{0.9}$ glass. Thermochim Acta. 2007;466:13.

14. Pérez–Maqueda LA, Criado JM, Málek J. Combined kinetic analysis for crystallization kinetics of non-crystalline solids. J Non-Cryst Solids. 2003;320:84.

15. Budrugeac P, Criado JM, Gotor FJ, Málek J, Pérez–Maqueda LA, Popescu C, Segal E. On the evaluation of the non–isothermal kinetic parameters of $(GeS_2)_{0.3}$ $(Sb_2S_3)_{0.7}$ crystallization using IKP method. Int J Chem Kinetics. 2004;36:209.

16. Málek J, Švadlák D, Mitsuhashi T, Haneda H. Kinetics of crystal growth of Sb_2S_3 in $(GeS_2)_{0.3}(Sb_2S_3)_{0.7}$ glass. J Non-Cryst Solids. 2006;352:2243–2253.

17. Švadlák D, Pustková P, Košťál P, Málek J. Crystal growth kinetics in $(GeS_2)_{0.2}(Sb_2S_3)_{0.8}$ glass. Thermochim Acta. 2006;446:121.

18. Švadlák D, Zmrhalová Z, Pustková P, Málek J, Pérez–Maqueda LA, Criado JM. Crystallization behavior of $(GeS_2)_{0.1}(Sb_2S_3)_{0.9}$ glass. J Non-Cryst Solids. 2008;354:3354.

19. Švadlák D. Crystallization kinetics in amorphous systems. Ph.D. Thesis, University of Pardubice; 2008.

20. Uhlmann DR, In: Hench LL, Freiman SW, editors. Advances in nucleation and crystallization in glasses. Columbus: American Ceramic Soc; 1972.

21. Jackson KA, Uhlmann DR, Hunt JD. On the nature of crystal growth from the melt. J Cryst Growth. 1967;1:1.

22. Johnson GK, Papatheodorou GN, Johnson CE. The enthalpies of formation of $SbF_5(1)$ and $Sb_2S_3(c)$ and the high-temperature thermodynamic functions of $Sb_2S_3(c)$ and $Sb_2S_3(l)$. J Chem Thermodyn. 1981;13:745.

23. Shánělová J, Košťál P, Málek J. Viscosity of $(GeS_2)_x(Sb_2S_3)_{1-x}$ supercooled melts. J Non-Cryst Solids. 2006;352:3952.

24. Woodruff DP. The solid-liquid interface. Cambridge: Cambridge University Press; 1973.